Derivation of high-order advection–diffusion schemes

Pavel Tkalich

ABSTRACT

Using the interpolation polynomial method, major upwind explicit advection–diffusion schemes of up to fifth-order accuracy are rederived and their properties are explored. The trend emerges that the higher the order of accuracy of an advection scheme, the easier is the task of scheme stabilization and wiggling suppression. Thus, for a certain range of the turbulent diffusion coefficient, the stability interval of third- and fifth-order up-upwind explicit schemes can be extended up to three units of the Courant number ($0 \leq c \leq 3$).

Having good phase behavior, advection odd-order schemes are stable within a single computational cell ($0 \leq c \leq 1$). By contrast, even-order schemes are stable within two consecutive grid-cells ($0 \leq c \leq 2$), but exhibit poor dispersive properties. Stemming from the finding that considered higher-order upwind schemes (even, in particular) can be expressed as a linear combination of two lower-order ones (odd in this case), the best qualities of odd- and even-order algorithms can be blended within mixed-order accuracy schemes. To illustrate the idea, a Second-Order Reduced Dispersion (SORD) marching scheme and Fourth-Order Reduced Dispersion (FORD) upwind scheme are developed. Computational tests demonstrate a favorable performance of the schemes. In spite of the previous practice restricting usage of even-order upwind schemes (fourth-order in particular), they exhibit a potential to stand among popular algorithms of computational hydraulics.

Key words | advection–diffusion, FORD, high-order upwinding, reduced dispersion, SORD

Pavel Tkalich
Tropical Marine Science Institute,
National University of Singapore,
14 Kent Ridge Road, Singapore 119223,
Singapore
E-mail: *tmspt@nus.edu.sg*

NOMENCLATURE

$\boldsymbol{A}$	matrix of known coefficients
a_{mk}	components of matrix $\boldsymbol{A}$
a	coefficient
$\boldsymbol{B}$	unknown vector, has to be identified
b_{m}	components of vector $\boldsymbol{B}$
c	Courant numbers
d	diffusion coefficient
$E_1, \ldots, E_4$	expressions for third-order up-upwind scheme
f_B	Dirichlet boundary condition
f'_B	Neumann boundary condition
G	amplification factor
g	amplitude of the Fourier component
I	imaginary number
i	node number
K	wavenumber
M	degree of the polynomial
n	time-level
P	polynomial in space domain
$\boldsymbol{S}$	computational stencil
T	polynomial in time domain
t	time coordinate
u	velocity
x	space coordinate
α	normalized local space coordinate
β	normalized local time coordinate
γ	convex variable
Δt	time-step
Δx	grid-size
δ	diffusion number
ε	error measure
θ	phase angle

doi: 10.2166/hydro.2006.008

ν	parameter
ϕ	transported scalar
ϕ'	pseudo-gradient of the transported scalar

SUBSCRIPTS

a	index of arrival point
adv	index of advection scheme
d	index of departure point
dif	index of diffusion scheme
i	index of node number
k, m	positive integer indices
r, l	index of right- and left-face values of the grid-cell
L, G	indices of local and global Courant number
s	index of velocity direction (± 1)

SUPERSCRIPTS

(M)	index of polynomial's degree
n	index of time-level
$*$	index of exact solution
0	index of initial condition

INTRODUCTION

Computational hydraulics pays special attention to an accurate solution of the model advection–diffusion equation for a scalar $\phi(t, x)$:

$$\frac{\partial \phi}{\partial t} + \frac{\partial u\phi}{\partial x} = \frac{\partial}{\partial x}\left(\mathrm{d}\frac{\partial \phi}{\partial x}\right) \tag{1}$$

where u is the advecting velocity, d is the turbulent diffusion coefficient, x is the space coordinate and t is the time. A conservative control-volume form of Equation (1) can be written as (Figure 1)

$$\phi_i^{n+1} = \phi_i^n - (c_r\phi_r - c_l\phi_l) + (\delta_r\phi_r' - \delta_l\phi_l') \tag{2}$$

where ϕ_i^n is the cell-averaged value of the transported scalar ϕ at the ith computational cell at time-level n, ϕ_r and ϕ_l are the right- and left-face values of the transported scalar for the ith cell, ϕ_r' and ϕ_l' are the right- and left-face

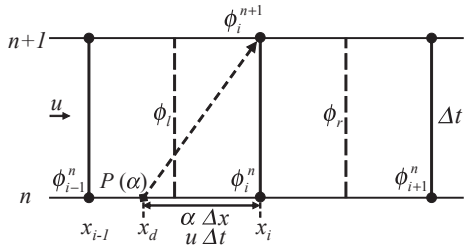

Figure 1 | Sketch of the semi-Lagrangian technique for positive u (as shown).

pseudo-gradient values of the scalar ϕ; $c_r\phi_r$, $c_l\phi_l$ and $\delta_r\phi_r'$, $\delta_l\phi_l'$ are the right- and left-face advective and diffusive fluxes, respectively, c_r and c_l are the right- and left-face values of the Courant number, $c = |u|\Delta t/\Delta x$, Δt is the time step, Δx is the grid size, δ_r and δ_l are the right- and left-face values of the diffusion number, $\delta = d\Delta t/(\Delta x)^2$. Mass conservation by the update (2) is guaranteed if $c_l\phi_l(i) = c_r\phi_r(i-1)$ and $\delta_l\phi_l'(i) = \delta_r\phi_r'(i-1)$.

In particular, the transport equation (1) is used in environmental hydraulics to describe temporal and spatial dynamics of admixture concentration ϕ in the water column. In the presence of strong currents the advection term often dominates the diffusion one, imposing specific requirements on the accuracy of the numerical techniques employed. To obtain a physically relevant numerical solution, the magnitude of the approximation error of the advection term (the so-called numerical diffusion) must be lower than the magnitude of the tubulent diffusion term. Accuracy of the numerical solution can be improved by refining a computational grid or by increasing the order of accuracy of the advection term approximation. The grid refinement leads to an excessive usage of computational resources. Therefore *for a prescribed global accuracy, higher-order methods are more computationally economical* (Leonard 1984).

The majority of popular explicit advection schemes are stable for $0 \le c \le 1$, the restriction known as the Courant–Friedrichs–Lewy or CFL condition (Courant *et al.* 1928). *Implicit schemes can extend the stability interval beyond the CFL condition, but the obtained solution may suffer from high numerical diffusion*, reducing efforts spent on implementation of the higher-order approximation. Explicit methods with added diffusion may be a good alternative to implicit algorithms, considering that *explicit methods are*

less expensive per time-step of computation. One well known example of such a scheme is the QUICK algorithm (Leonard 1979), which is unstable for a pure advection but is conditionally stable for the advection–diffusion case.

The significance of even-order upwind explicit schemes has been long underestimated. Studying high-order approximations, Leonard (1984) in particular stated that, since second- (and forth-) order accuracy upwind methods are too dispersive, and since fifth- and higher-order methods are excessively complex, the third-order upwinding (QUICKEST algorithm) forms a rational basis for Computational Fluid Dynamics (CFD). One important property was not fully considered in the statement, but discussed by Leonard (2002) much later, namely *even-order schemes have a two times wider stability interval than odd-order ones*. Thus, the well known explicit second-order upwinding (Warming & Beam 1976) is stable at the extended interval $0 \leq c \leq 2$.

Higher- (than first-)order advection schemes provide a non-monotonic solution having unphysical oscillations (wiggling) in the vicinity of sharp gradients of the transported scalar ϕ. If the wiggling is not severe, *the diffusion term or intentionally added numerical diffusion may effectively smooth out and/or stabilize the high-order approximation*. This is especially useful for water quality problems, where the value of the turbulent diffusion coefficient d can be quite high. In other cases, certain modifications to the original high-order scheme can be made (the so-called flux limiters (Boris & Book 1973; Van Leer 1974; Zalesak 1979)), suppressing spurious oscillations without corrupting the expected accuracy of the underlying method. At the present time, due to the research of Roe (1986), Leonard & Mokhtari (1990), Li & Rudman (1995) and many others, application of flux limiters is becoming common. *Flux limiters perform as efficient in combination with even-order approximations as they do with odd-order schemes*.

The introduction can be summarized as follows. Since lower-than-third-order-accuracy schemes are too inaccurate for the transport processes, and since fourth-order schemes have wider stability intervals than third-order ones, and since fifth- and higher-order upwind methods are excessively complex, and since the compulsory diffusion term is smoothing out and stabilizing the solution, and since optional flux limiters are equally effective for odd and even high-order schemes, and since explicit methods are more effective than implicit per time-step of computation, one can conclude that: *fourth-order upwind explicit schemes have a potential to stand among the popular advection algorithms of computational hydraulics*.

This paper reviews major upwind explicit schemes for accurate simulation of advection and diffusion. The basics of the numerical method's derivation using polynomial approximations are elaborated. Schemes of up to fifth-order accuracy are rederived, their hierarchical linkage is established and stability patterns and trends are analyzed. Application of diffusion approximations may help to improve the stability and dispersion properties of advection schemes. The trend emerges that the higher the order of accuracy of an advection approximation, the easier is the task of scheme stabilization. Thus, a stability interval of third- and fifth-order up-upwind explicit schemes can be extended for up to three units of the Courant number ($0 \leq c \leq 3$). A new class of mixed-order advection schemes that inherits improved dispersion behavior of odd-order methods and the extended stability criterion of even-order ones is suggested. Two new mixed-high-order schemes (SORD and FORD) are developed. All methods considered are compared with well known algorithms using test cases and analytical solutions.

DERIVATION OF NUMERICAL SCHEMES USING THE POLYNOMIAL APPROXIMATION

To remain within the finite-volume approach (2), one can apply the flux integral method, as in Leonard *et al.* (1995), to obtain scalar values and gradients (and respective "true" fluxes $c_r\phi_r$, $c_l\phi_l$ and $\delta_r\phi_r'$, $\delta_l\phi_l'$) at the right- and left-faces of the control-volume i. Alternative methods, such as one developed in this paper, may lead to pseudo-fluxes, with formulation (2) being interpreted as a conservative finite-difference update; though, in many cases, the pseudo-fluxes may coincide with the "true" fluxes. The difference between the two approaches is discussed extensively by Leonard (1995, 2002).

Advection term approximation

For pure advection ($d = 0$), the semi-Lagrangian technique yields an exact solution of Equation (1) over time Δt as (Figure 1)

$$\phi_i^{n+1} = \phi(t^n + \Delta t, x_i) = \phi(t^n, x_i - u\Delta t) \tag{3}$$

expressing the concept that any distribution at time-level t^n is advected to time-level t^{n+1} without changing its form. The transported scalar ϕ at the point $(t^n, x_i - u\Delta t)$ is approximated using a piecewise interpolation polynomial

$$P^{(M)}(\alpha) = \sum_{m=0}^{M} \alpha^m b_m \tag{4}$$

where $\alpha = (x_i - x_d)/\Delta x$ is the normalized local coordinate and M is the degree of the polynomial. Unknown coefficients $\mathbf{B} = \{b_m\}$ depend on values of the transported scalar ϕ at nodes of the computational stencil $\mathbf{S} = \{\phi_k^n\}$. To define uniquely $M+1$ coefficients $\{b_m\}$ using Lagrange polynomial elements, $M+1$ linear equations have to be derived requiring that the polynomial passes through every node from the computational stencil $\mathbf{S}$, i.e.

$$\sum_{m=0}^{M} a_{mk} b_m = \phi_k^n, \quad k = 0, 1, \ldots, M. \tag{5}$$

A matrix form of Equation (5) is $\mathbf{AB} = \mathbf{S}$, where components of the matrix $\mathbf{A} = \{a_{mk}\}$ are known and the vector $\mathbf{B}$ has to be identified. Solution of the system (5) can be obtained by finding the inverse matrix $\mathbf{A}^{-1}$, and then $\mathbf{B} = \mathbf{A}^{-1}\mathbf{S}$. To define a unique solution of Equations (5), the number of nodes in the computational stencil has to be $M+1$.

Finally, combining Equations (3) and (4), and substituting found coefficients $\{b_m\}$, one obtains the explicit single-step update

$$\phi_i^{n+1} = P^{(M)}(\alpha) \tag{6}$$

where α coincides with the Courant number c for positive u. To match the control-volume form (Equation (2)), the right-face flux can be derived equalizing right-hand sides of Equations (2) and (6), leading to $(c_r\phi_r)_i = \phi_i^n - P^{(M)}(c) + (c_r\phi_r)_{i-1}$. If velocity values are specified at the same nodes as the transported scalar ϕ, one may assume $c = (c_r)_i = |u_i|\Delta t/\Delta x$.

Diffusion term approximation

The diffusion term in Equation (1) can be approximated numerically using a second x derivative of the transported scalar ϕ (Equation (6)) at the point (t^{n+1}, x_i), i.e.

$$\left.\frac{\partial^2\phi}{\partial x^2}\right|_{(t^{n+1},x_i)} = \frac{1}{(\Delta x)^2}\frac{\partial^2 P^{(M)}(\alpha)}{\partial \alpha^2} = \frac{1}{(\Delta x)^2}\sum_{m=0}^{M} m(m-1)\alpha^{m-2} b_m, \quad (M \geq 2)$$

To satisfy the control volume form (2), the right-face diffusive flux has to follow

$$(\delta_r\phi_r')_i = \frac{\partial}{\partial\alpha}\delta\frac{\partial P^{(M)}(\alpha)}{\partial\alpha} + (\delta_r\phi_r')_{i-1}. \tag{7}$$

If values of the diffusion coefficient d are specified at the same nodes as the transported scalar ϕ, one assumes $(\delta_r)_i = 0.5(\delta_i + \delta_{i+1})$. For first-degree polynomials any standard diffusion approximation can be applied, such as the Forward-Time-Central-Space (FTCS) scheme (Roache 1976) with the right-face flux $(\delta_r\phi_r')_i = 0.5(\delta_i + \delta_{i+1})(\phi_{i+1}^n - \phi_i^n)$.

Stability analysis

It is instructive to obtain stability criteria of any newly developed numerical scheme. According to the von Neumann stability analysis, the solution of Equation (6) is sought in the form $\phi_i^n = g^n \exp(Ii\theta)$, where $\theta = K\ \Delta x$ is the phase angle, g^n is the amplitude of the Fourier component at $n\Delta t$, K is the wavenumber and $I = \sqrt{-1}$. A difference scheme is considered stable for a chosen value of the Courant number c if a modulus of the amplification factor, G, is less or equal to unity for all phase angles θ over one complete time-step, i.e., $|G(\theta, c)| = |g^{n+1}/g^n| \leq 1$. Further in this paper, the amplification factor for the reviewed schemes is computed and analyzed graphically for the special case of uniform flow and grid (α = constant, δ = constant).

Test case

A series of numerical tests is performed to compare the performance of the schemes presented in this paper. In one of the tests, an idealized 1D computational domain consists of 10,000 nodes, numbered from left to right, with the grid-size $\Delta x = 100$ m. A uniform velocity $u = 1$ m/s is set in the entire domain. Initial values of the transported scalar are set to zero in the entire domain, except for the interval (150 Δx,

250 Δx), where $\phi^0 = 1$. It is expected that for pure advection an ideal numerical scheme does not introduce a distortion into the initial shape, while moving it with the flow. Computations are conducted to allow the initial profile to advect to the opposite side of the domain, where the final profile is compared with an exact solution, and the error measure is computed using the relationship

$$\varepsilon = \frac{\sum_{i,j}\left|\phi_i - \phi_i^*\right|}{\sum_{i,j}\left|\phi_i^*\right|} \tag{8}$$

where $\phi*$ is the exact solution and ϕ is the numerical one.

HIERARCHY OF UPWIND NUMERICAL SCHEMES

In this section major upwind advection explicit schemes are rederived using the interpolation polynomials of up to fifth degree and a recursive hierarchy of the algorithms is established. The schemes are compared in Figure 2 and Table 1 using the test case, and plots of the modulus $|G(\theta, c)|$ are given in Figures 3 and 4. Boundaries of regions where $|G| < 1$ are marked with shading. The derived advection schemes (single-step updates) are supplemented with

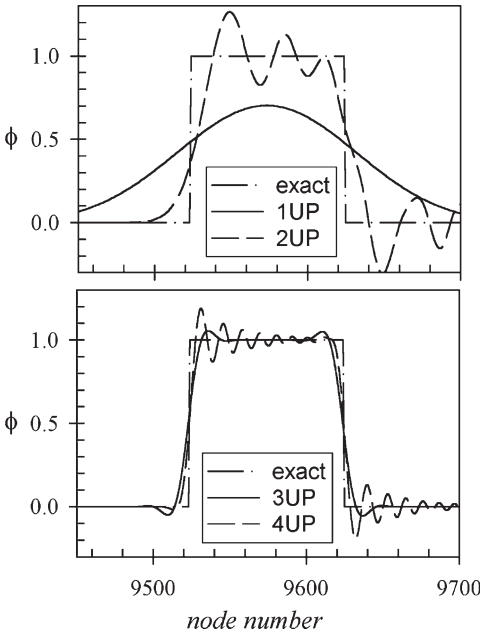

Figure 2 | Comparison of some upwind advection schemes: first- (1UP), second- (2UP), third- (3UP or QUICKEST) and fourth-order (4UP). $c = 0.75$.

right-face advective and diffusive fluxes (given in the Appendix). Once combined, advection–diffusion schemes form effective one-step algorithms for solution of the transport equation.

For the first-degree polynomial ($M = 1$ in Equation (4)) defined at the interval $[x_{i-1}, x_i]$ for $u > 0$, or at $[x_i, x_{i+1}]$ for $u < 0$, the first-order upwind update follows:

$$(\phi_i^{n+1})_{adv}^{1UP} = (1 - c)\phi_i^n + c\phi_{i-s}^n \tag{9}$$

where $s = 1$ for $u > 0$, and $s = -1$ otherwise. The method is stable at the single grid-cell $[x_{i-s}, x_i]$, leading to the stability condition $0 \le c \le 1$ (Figure 3(a)). For future reference, two more first-order advection updates are derived: downwind

$$\left(\phi_i^{n+1}\right)_{adv}^{1DN} = (1 - c)\phi_i^n + c\phi_{i+s}^n$$

and up-upwind

$$\left(\phi_i^{n+1}\right)_{adv}^{1UU} = (2 - c)\phi_{i-s}^n - (1 - c)\phi_{i-2s}^n.$$

For the second-degree polynomial ($M = 2$ in Equation (4)), two popular second-order methods follow, both belong to the class of Lax–Wendroff schemes (Lax & Wendroff 1960 1964). The central differencing advection update at the nodes (x_{i-1}, x_i, x_{i+1}) is given by Leith (1965) as

$$\left(\phi_i^{n+1}\right)_{adv}^{2CN} = -\left[\frac{1}{2}c(1 - c)\right]\phi_{i+1}^n + \left[1 - c^2\right]\phi_i^n + \left[\frac{1}{2}c(1 + c)\right]\phi_{i-1}^n. \tag{10}$$

Similarly, using nodes (x_{i-2s}, x_{i-s}, x_i) the second-order upwinding follows

$$\left(\phi_i^{n+1}\right)_{adv}^{2UP} = \left[\frac{1}{2}(1 - c)(2 - c)\right]\phi_i^n + \left[c(2 - c)\right]\phi_{i-s}^n - \left[\frac{1}{2}c(1 - c)\right]\phi_{i-2s}^n. \tag{11}$$

The schemes (10) and (11) are stable at the intervals $[x_{i-1}, x_{i+1}]$ and $[x_{i-2s}, x_i]$ (two grid-cells each), yielding the stability conditions $-1 \le c \le 1$ and $0 \le c \le 2$, respectively (Figure 4(a)).

The third-degree polynomial (4) at nodes $(x_{i-2s}, x_{i-s}, x_i, x_{i+s})$ leads to the upwind scheme (3UP) known also as the

Table 1 | Comparison of properties of different advection schemes using the test case for $c = 0.75$

		SORD					
Advection schemes	**1UP**	**$\nu = 1$**	**$\nu = 0$**	**2UP**	**QUICKEST (3UP)**	**FORD**	**4UP**
Error measure, ε	0.738	0.519	0.254	0.350	0.091	0.074	0.117
$\phi_{\max}$	0.713	1.275	1.004	1.266	1.055	1.110	1.189
$\phi_{\min}$	0.000	−0.333	−0.004	−0.296	−0.055	−0.110	−0.194

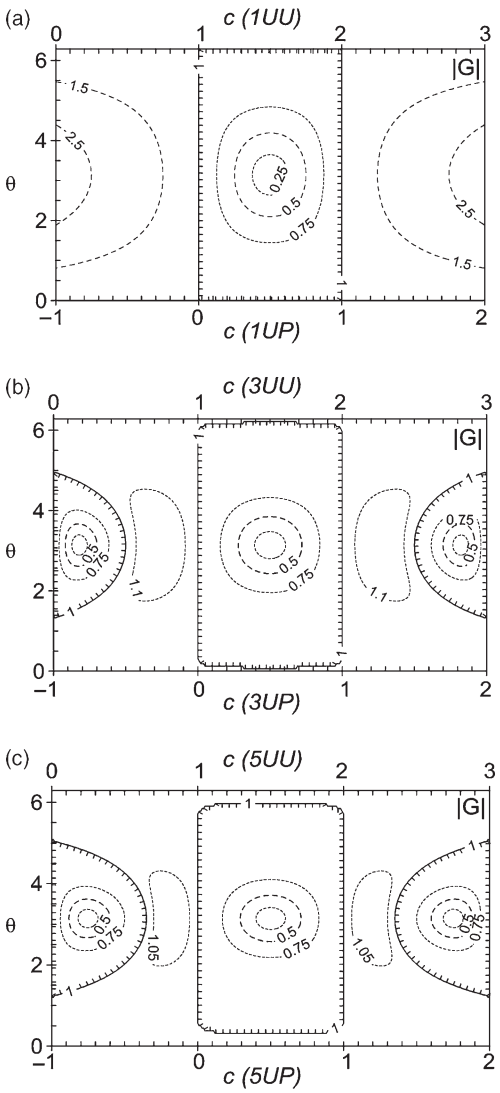

Figure 3 | Two-dimensional plot of the amplification factor modulus, $|G(\theta, c)|$, for advection schemes: (a) first-order; (b) third-order; (c) fifth-order. Boundaries of the stability regions are marked with shading.

QUICKEST (Leonard 1979):

$$\left(\phi_i^{n+1}\right)_{adv}^{3UP} = -\left[\frac{1}{6}c(1-c)(2-c)\right]\phi_{i+s}^n + \left[\frac{1}{2}(1-c^2)(2-c)\right]\phi_i^n + \left[\frac{1}{2}c(1+c)(2-c)\right]\phi_{i-s}^n - \left[\frac{1}{6}c(1-c^2)\right]\phi_{i-2s}^n. \quad (12)$$

The same order polynomial at nodes $(x_{i-3s}, x_{i-2s}, x_{i-s}, x_i)$ yields the up-upwind scheme:

$$\left(\phi_i^{n+1}\right)_{adv}^{3UU} = \left[\frac{1}{6}(1-c)(2-c)(3-c)\right]\phi_i^n + \left[\frac{1}{2}c(2-c)(3-c)\right]\phi_{i-s}^n - \left[\frac{1}{2}c(1-c)(3-c)\right]\phi_{i-2s}^n + \left[\frac{1}{6}c(2-c)(1-c)\right]\phi_{i-3s}^n. \quad (13)$$

The third-order advection schemes (12) and (13) are stable at (single grid-cell) intervals $[x_{i-s}, x_i]$ and $[x_{i-2s}, x_{i-s}]$, leading to the stability conditions $0 \le c \le 1$ and $1 \le c \le 2$, respectively (Figure 3(b)).

The fourth-degree polynomial ($M = 4$ in Equation (4)) yields the fourth-order upwinding scheme:

$$\left(\phi_i^{n+1}\right)_{adv}^{4UP} = -\left[\frac{1}{24}c(1-c)(2-c)(3-c)\right]\phi_{i+s}^n + \left[\frac{1}{6}(1-c^2)(2-c)(3-c)\right]\phi_i^n + \left[\frac{1}{4}c(1+c)(2-c)(3-c)\right]\phi_{i-s}^n - \left[\frac{1}{6}c(1-c^2)(3-c)\right]\phi_{i-2s}^n + \left[\frac{1}{24}c(1-c^2)(2-c)\right]\phi_{i-3s}^n. \quad (14)$$

The scheme (14) is stable at the two-grid-cell interval $[x_{i-2s}, x_i]$ ($0 \le c \le 2$ as in Figure 4(b)). Finally, the fifth-order upwind and up-upwind schemes are stable, respectively, for $0 \le c \le 1$ and $1 \le c \le 2$, as in Figure 3(c). The fifth-order

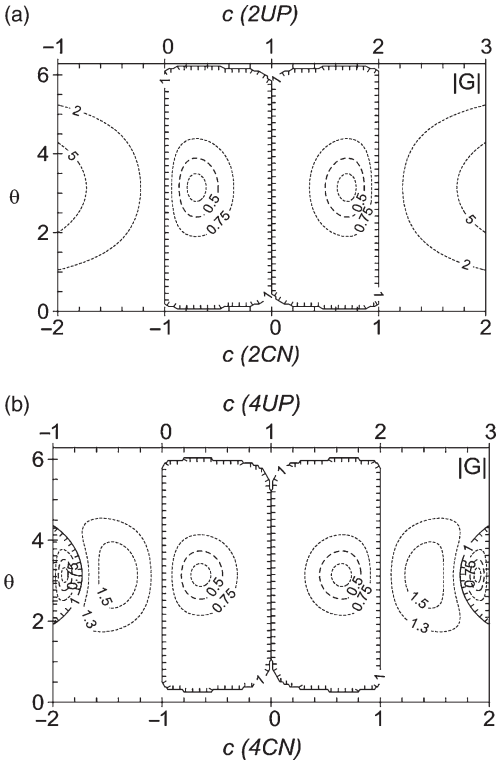

Figure 4 | Two-dimensional plot of the amplification factor modulus, $|G(\theta, c)|$, for advection schemes: (a) second-order; (b) fourth-order. Boundaries of the stability regions are marked with shading.

up-upwind scheme is

$$\begin{aligned}\left(\phi_i^{n+1}\right)_{adv}^{5UU} = &-\left[\frac{1}{120}c(1-c)(2-c)(3-c)(4-c)\right]\phi_{i+s}^n \\ &+\left[\frac{1}{24}(1-c^2)(2-c)(3-c)(4-c)\right]\phi_i^n \\ &+\left[\frac{1}{12}c(1+c)(2-c)(3-c)(4-c)\right]\phi_{i-s}^n \\ &-\left[\frac{1}{12}c(1-c^2)(3-c)(4-c)\right]\phi_{i-2s}^n \\ &+\left[\frac{1}{24}c(1-c^2)(2-c)(4-c)\right]\phi_{i-3s}^n \\ &-\left[\frac{1}{120}c(1-c^2)(2-c)(3-c)\right]\phi_{i-4s}^n.\end{aligned} \tag{15}$$

In spite of the complex appearance, the reviewed schemes can be coded quite efficiently, considering that expressions in square brackets have to be recomputed only if the velocity u has changed with time. Summarizing stability regions of the considered advection schemes it is clear that first-, third- and higher-odd-order algorithms are stable within a single grid-cell, leading to the conventional CFL condition, $0 \le c \le 1$; while second-, fourth- and higher-even-order ones are stable at two consecutive grid-cells, giving the extended stability condition, $0 \le c \le 2$. The computational tests (Figure 2 and Table 1) confirm the previously known phenomenon (Leonard 1984, 2002) that even-order schemes result in dispersive algorithms having spurious trailing oscillations. In contrast, odd-order methods have much better phase behavior. Further increase of the interpolant's degree (and order of approximation, respectively) just slightly improves the accuracy of the resulting scheme, but algorithms become more and more computationally expensive.

Analyzing the derived advection approximations, one may notice that higher-order schemes can be expressed via a linear combination of two lower-order ones. Thus, the second-order central scheme becomes

$$\left(\phi_i^{n+1}\right)_{adv}^{2CN} = \left(1-\gamma\right)\left(\phi_i^{n+1}\right)_{adv}^{1DN} + \gamma\left(\phi_i^{n+1}\right)_{adv}^{1UP}, \quad \text{for} \quad \gamma = (1+c)/2$$

and the second-order upwinding is

$$\left(\phi_i^{n+1}\right)_{adv}^{2UP} = (1-\gamma)\left(\phi_i^{n+1}\right)_{adv}^{1UP} + \gamma\left(\phi_i^{n+1}\right)_{adv}^{1UU}, \quad \text{for} \quad \gamma = c/2.$$

A similar dependence is valid for the third-order schemes, i.e.

$$\left(\phi_i^{n+1}\right)_{adv}^{3UP} = \left(1-\gamma\right)\left(\phi_i^{n+1}\right)_{adv}^{2CN} + \gamma\left(\phi_i^{n+1}\right)_{adv}^{2UP}, \quad \text{for} \quad \gamma = (1+c)/3 \tag{16}$$

and

$$\left(\phi_i^{n+1}\right)_{adv}^{3UU} = \left(1-\gamma\right)\left(\phi_i^{n+1}\right)_{adv}^{2UP} + \gamma\left(\phi_i^{n+1}\right)_{adv}^{2UU}, \quad \text{for} \quad \gamma = c/3.$$

For the particular case of $\gamma = 0.5$, a consideration similar to Equation (16) was used by Fromm (1968) to derive his "zero-average phase error" method. Observing that the central scheme 2CN has a predominantly lagging phase error at the interval $0 \le c \le 1$ and the upwinding 2UP has a leading error at the same interval, the author merged the two methods to obtain a provisionally third-order scheme having improved dispersion behavior. Interestingly, Equation (16) represents

an alternative interpretation of the QUICKEST algorithm as being a convex combination of two second-order schemes.

Expressing Equation (14) as a linear combination of two third-order schemes, one gets

$$\left(\phi_i^{n+1}\right)_{adv}^{4UP} = \left(1-\gamma\right)\left(\phi_i^{n+1}\right)_{adv}^{3UP} + \gamma\left(\phi_i^{n+1}\right)_{adv}^{3UU}, \quad \text{for } \gamma = (1+c)/4. \tag{17}$$

Following the developed recursive routine, upwind algorithms are extendable to higher and higher order, with an arbitrary $(M+1)$th-order scheme being a linear interpolation of two Mth-order ones as

$$\left(\phi_i^{n+1}\right)_{adv}^{(M+1)UP} = \left(1-\gamma\right)\left(\phi_i^{n+1}\right)_{adv}^{MUP} + \gamma\left(\phi_i^{n+1}\right)_{adv}^{MUU}, \text{for } \gamma = (1+c)/(M+1). \tag{18}$$

Equation (18) offers a simple derivation technique for arbitrary-order advection schemes.

COURANT-NUMBER-EQUAL-TO-OR-LESS-THAN-ONE CONDITION

The original CFL condition (Courant *et al.* 1928) states that in a numerical grid which does not follow the characteristic directions, the finite-difference domain of dependence must at least include the continuum domain of dependence. Due to some of the earliest applications of computational science, the condition was narrowly interpreted as $0 \le c \le 1$ for explicit schemes, and the restriction became a sort of psychological barrier ever since. Interestingly, the second-order upwind scheme, known to satisfy the extended stability condition $0 \le c \le 2$, has often been considered as the exception to the Courant-number-less-than-one "fundamental" rule. Among major attempts to overcome the $c = 1$ barrier are semi-Lagrangian (characteristic) methods, in which the trajectory's arrival point (t^{n+1}, x_a) can became separated from the computational stencil containing the trajectory's departure point (t^n, x_d), as in Figure 5. Here and later some terminology of Leonard (2002) is utilized. Since the distance between the departure and arrival points does not affect the stability of the resulting algorithm, one might claim that the schemes are stable for an arbitrary Courant number.

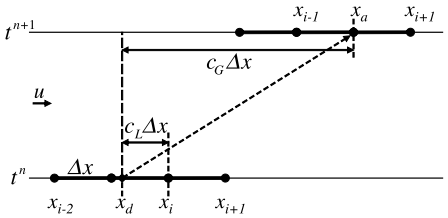

Figure 5 | Sketch of semi-Lagrangian methods for positive u (as shown); c_G and c_L are the "global" and "local" Courant numbers, respectively.

Clearly, there is a confusion between the "local" Courant number, having its origin at the balance point (t^n, x_i), defined at the center of the spatial stencil in index space, and the "global" Courant number with the origin at the arrival point. Even though many Eulerian schemes mentioned in this paper can be reformulated for an arbitrary Courant number in the global sense (as was done by Leonard (2002)), both, Eulerian and semi-Lagrangian schemes still bear the same classical restriction $0 \le c \le 1$ or $0 \le c \le 2$ in the local sense.

Roache (1992) gave a more relevant, and yet general, interpretation of the CFL condition that the explicit upwind method must interpolate (within the stencil), not extrapolate, to compute a value at the departure point. That is, the characteristic which ended up at the time-level $(n+1)$ must originate within the same computational stencil at the time-level n. Leonard (2002) formulated a more strict, but necessary and sufficient, condition for stability as "the balance point must be located in the same patch/cell as the departure/sweep point". This definition limits the stability interval to one or two patches/cells, depending on an order (odd or even) of the scheme; which in terms of "local" Courant number leads to the classical condition $0 \le c \le 1$ or $0 \le c \le 2$, respectively.

In large-Courant-number semi-Lagrangian schemes one can trace back the departure interval from the arrival point using an averaged velocity value. The correct averaging procedure has to include velocities from all nodes along the trajectory; otherwise, an attempt to use values from an estimated departure interval may only lead to multiple solutions, as shown in an example with non-uniform velocities presented in Appendix C. Hence, maintenance of mass conservation properties in semi-Lagrangian schemes with non-uniform velocities may present an enormous challenge. One solution to the problem would

be the use of large-Courant-number schemes with the arrival point remaining within the departure stencil (as in Eulerian schemes). To extend the CFL condition beyond the unit Courant number, Eulerian schemes must be modified to use longer computational stencils with the extended stability interval. One may wonder whether the interval can be extended at the entire computational stencil for higher-order schemes, as it is for the first- and second-order ones. The next section suggests a method of extending the stability criteria by means of explicitly added turbulent diffusivity.

INFLUENCE OF DIFFUSIVITY ON THE SCHEME STABILITY

Analyzing the amplification factor plots for different schemes in Figures 3 and 4, it is clear that, as the order of accuracy increases, a maximal value of $|G|$ tends down towards unity; or, as one might say, the instability becomes "weaker". Therefore, the higher the order of the scheme, the easier is the task of scheme stabilization. Explicitly added physical or numerical diffusivity is a common way to improve the stability. QUICK (Leonard 1979) is the well known example of such a scheme: it is unstable for a pure advection and is conditionally stable if the parabolic term is present. Although the majority of admixture transport problems in water bodies contain the diffusion term to account for molecular and turbulent diffusion, the magnitude of the diffusion coefficient may not be sufficient to stabilize an unstable advection scheme. In such cases, one usually is advised to use an implicit advection scheme instead of explicit, even though implicit algorithms are less efficient than a single-node computation. Increasing the time-step seems to make implicit algorithms more efficient than explicit, but the schemes may suffer loss of accuracy, which deteriorates rapidly once the departure point separates from the computational stencil. This is due to an inefficient approximation of the transported scalar using values from two time-levels. According to the evaluation of Roache (1992) for the first-order upwinding, when the time-step increased 10 times (from $c = 0.5$ for explicit to $c = 5$ for implicit schemes) the numerical diffusivity increased 12 times. That is, the implicit algorithms gain stability at large time-steps by imposing the progressively increasing numerical diffusion, and solutions are becoming so diffusive that higher-order advection schemes may lose their advantage over the lower-order ones. To be effective, high-order schemes (implicit and explicit) must satisfy Roache's interpretation of the CFL condition to interpolate. Such a limitation may diminish the benefits of implicit methods because the same time-step range, hopefully, can be achieved by more efficient explicit schemes. Therefore, the challenge is to extend the stability interval of explicit schemes to the entire computational stencil.

The third-order up-upwind scheme (3UU, Equation (13)) is a good object to demonstrate such a development. The scheme seems to be impractical due to the unconventional stability criterion, $1 \le c \le 2$ (see Figure 3(b)). Taking into account that the instability is relatively "weak" j($|G|_{\max} = 1.188$) at the intervals $0 \le c \le 1$ and $2 \le c \le 3$, there is a possibility of making the scheme stable for the entire range $0 \le c \le 3$ by adding some explicit physical diffusivity. For the exploratory purpose the simplest (FTCS) diffusion scheme is used:

$$(\phi_i^*)_{dif} = \phi_i^n + \delta(\phi_{i+1}^n - 2\phi_i^n + \phi_{i-1}^n) \tag{19}$$

which is stable for $0 \le \delta \le 0.5$. Here, the symbol "$*$" indicates an intermediate scalar value at the new time-level. After simplifying the notation of expression (13) as

$$\left(\phi_i^{n+1}\right)_{adv-dif}^{3UU} = \left[E_1\right](\phi_i^*)_{dif} + \left[E_2\right]\left(\phi_{i-s}^*\right)_{dif} + \left[E_3\right] \times \left(\phi_{i-2s}^*\right)_{dif} + \left[E_4\right]\left(\phi_{i-3s}^*\right)_{dif} \tag{20}$$

Equation (19) has to be substituted into Equation (20) to yield the combined advection–diffusion scheme:

$$\begin{aligned}\left(\phi_i^{n+1}\right)_{adv-dif}^{3UU} =& E_1\delta\phi_{i+s}^n + \left[E_1(1-2\delta) + E_2\delta\right]\phi_i^n \\ &+ \left[E_1\delta + E_2(1-2\delta) + E_3\delta\right]\phi_{i-s}^n \\ &+ \left[E_2\delta + E_3(1-2\delta) + E_4\delta\right]\phi_{i-2s}^n \\ &+ \left[E_3\delta + E_4(1-2\delta)\right]\phi_{i-3s}^n + E_4\delta\phi_{i-4s}^n.\end{aligned}$$

Numerical investigation of the scheme's stability for the test case (Figure 6(a)) shows the expected features: being

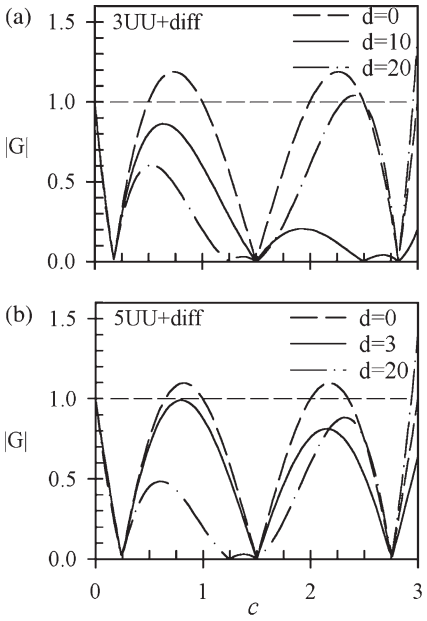

Figure 6 | Modulus of amplification factor for some advection schemes with the diffusion term: (a) third-order up-upwinding (3UU); (b) fifth-order up-upwinding (5UU). $\theta = \pi$, $\Delta x = 100$ m. The FTCS diffusion scheme is used. Values of the diffusion coefficient are shown in (m^2/s). Solid lines are with respect to stable solutions at $0 \le c \le 3$.

unstable for $d = 0$ out of the interval $1 \le c \le 2$, the scheme becomes stable at $0 \le c \le 3$ after $d > 9\,m^2/s$ and remains so until $\delta = 0.5$ ($d \approx 17\,m^2/s$ at $c = 3$). The combined scheme demonstrates a uniformly good performance for different values of the Courant number from the interval $0 \le c \le 3$ (Figure 7). Comparing the accuracy of the third-order up-upwind advection–diffusion scheme ($\phi_{max} = 0.75$) with the first-order upwind advection scheme (Equation (9), $\phi_{max} = 0.70$ in Figure 2), it is clear that the numerical

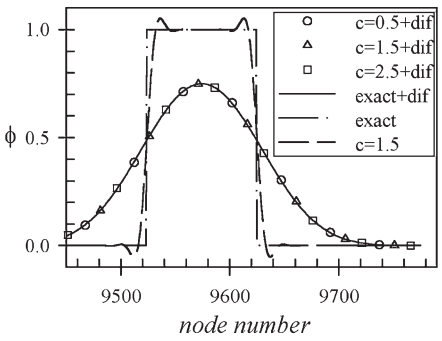

Figure 7 | Solution of the transport equation for different values of the Courant number using the third-order up-upwind (3UU) approximation for advection term and the FTCS scheme for diffusion term ($d = 10\,m^2/s$). The exact advection solution is referred to as "exact". Advection–diffusion solutions are identified with "+ dif".

diffusion of the first-order upwinding is higher than the explicitly introduced physical diffusion of the third-order advection–diffusion scheme. However, the extended stability of the third-order upwinding would be not possible for a smaller diffusivity.

Recalling that the instability is "weakening" when an order of approximation is increasing (Figure 3), it is expected that the fifth-order up-upwind scheme (15) may become stable at a wider range of the diffusion coefficient. Indeed, the maximum of the amplification factor modulus for the algorithm (15) is just $|G|_{max} = 1.098$ (Figure 3(c)) and the combined fifth-order up-upwinding–FTCS diffusion scheme is becoming stable for the entire interval $0 \le c \le 3$ once the diffusion coefficient exceeds the value $d \ge 3\,m^2/s$ (for the test case, Figure 6(b)). The typical stability limitation $0 \le \delta \le 0.5$ for the FTCS is still valid for the combined scheme.

MIXED-ORDER ADVECTION SCHEMES

Generalizing features of the advection algorithms considered above, one recalls that odd-order schemes have excellent phase behavior, but are stable only for $0 \le c \le 1$ in the local sense; at the same time, even-order schemes are stable for $0 \le c \le 2$, but have a poor phase behavior. This leads to controversial requirements that an ultimate explicit upwind scheme should be of even-order accuracy for a wider stability range, and of odd-order for better dispersive behavior. A possible solution is suggested in this section following the finding that the schemes reviewed can be expressed via a linear interpolation of two lower-order ones, as shown by Equation (18). Indeed, manipulating with the interpolation variable γ, there is a prospect to find mixed-order algorithms, that can achieve both: the extended stability range of even-order schemes and the improved dispersive behavior of constituent odd-order ones. Illustrating the idea, two new mixed-order schemes are developed. To hint at the remote origin of the schemes, they are identified as SORD (Second-Order Reduced Dispersion) and FORD (Fourth-Order Reduced Dispersion), though the order of accuracy depends on the value of the interpolation variable γ.

Second-Order Reduced Dispersion (SORD) scheme

It is possible to extend the derivation technique (Equation (18)) to the development of marching schemes, also known as Alternating Direction Explicit (ADE) methods (Roache 1976). Consider application of the semi-Lagrangian technique for the case of a Courant number greater than one (as in Figure 8):

$$\phi_i^{n+1} = \phi(t^n, x_d) = T(\beta), \text{ for } u \geq \Delta x/\Delta t, \quad (21)$$

where $T(\beta)$ is the piecewise interpolation polynomial and $\beta = (t - t^n)/\Delta t$ is the normalized local coordinate. At the interval $[t^n, t^{n+1}]$ a first-degree polynomial can be defined as

$$T(\beta) = (1 - \beta)\phi_{i-1}^n + \beta\phi_{i-1}^{n+1}, \quad 0 \leq \beta \leq 1. \quad (22)$$

The local coordinate β is determined from simple geometrical considerations as $\beta = (c - 1)/c$ for $c \geq 1$. Substitution of Equation (22) into (21) leads to the first-order upwind marching (1UM) scheme

$$\left(\phi_i^{n+1}\right)^{1UM} = (1 - \beta)\phi_{i-1}^n + \beta\phi_{i-1}^{n+1} \quad (23)$$

stable at $1 \leq c \leq \infty$. Similar to the established procedure (18), interpolation between the two first-order upwind polynomials, 1UP (Equation (9)) and 1UM (Equation (23)), leads to a higher-order marching algorithm (tagged as the Second-Order Reduced Dispersion, SORD):

$$\left(\phi_i^{n+1}\right)_{adv}^{SORD} = \left(1 - \gamma\right)\left(\phi_i^{n+1}\right)^{1UP} + \gamma\left(\phi_i^{n+1}\right)^{1UM}, \quad \gamma = ac. \quad (24)$$

Here

$$a = \frac{1}{2}\left(1 + \nu\frac{1 - c}{1 + c}\right)$$

where the parameter $\nu\,(0 \leq \nu \leq 1)$ controls the accuracy and phase behavior of the scheme. For $\nu = 1$ the scheme reduces to the second-order accurate box method (Noye 1986); other cases $(0 \leq \nu < 1)$ lead to a more diffusive algorithm. Using the relationships (9) and (23), Equation (24) yields

$$\left(\phi_i^{n+1}\right)_{adv}^{SORD} = \left[(1 - c)(1 - ac)\right]\phi_i^n + \left[a + c - ac^2\right]\phi_{i-1}^n - \left[a(1 - c)\right]\phi_{i-1}^{n+1}. \quad (25)$$

A stability condition for SORD is found to be $c \leq 1 + 2(1 - \nu)^{-1/2}$. The criterion shows unconditional stability for $\nu = 1$, and is limited to $c \leq 3$ for $\nu = 0$. The amplification factor for different values of c and ν are plotted in Figure 9. Using the test case, SORD is compared with other well known schemes in Figure 10 and Table 1 for $\nu = 0$ and $\nu = 1$. The case $\nu = 1$ shows a poor phase behavior, typical for second-order schemes. The case $\nu = 0$ demonstrates intermediate behavior between first- and second-order accuracy and a good phase behavior. According to the required accuracy, one may chose any value of the parameter ν from the interval [0, 1]. To maintain the transportivity property, marching has to be organized in the flow direction; therefore marching schemes are most useful for the cases of unidirectional river flows.

Fourth-Order Reduced Dispersion (FORD) scheme

Analyzing fourth-order upwinding, Equation (17), it is clear that the interpolation variable ranges from $0.25 \leq \gamma \leq 0.75$, thus ensuring a comparable contribution of the constituent third-order schemes (3UP and 3UU) within the entire

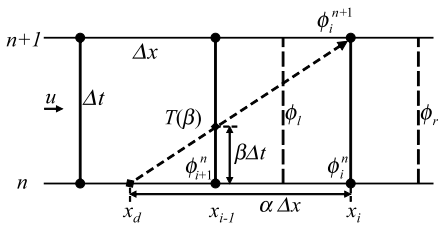

Figure 8 | Sketch of semi-Lagrangian technique for large Courant number and positive u (as shown).

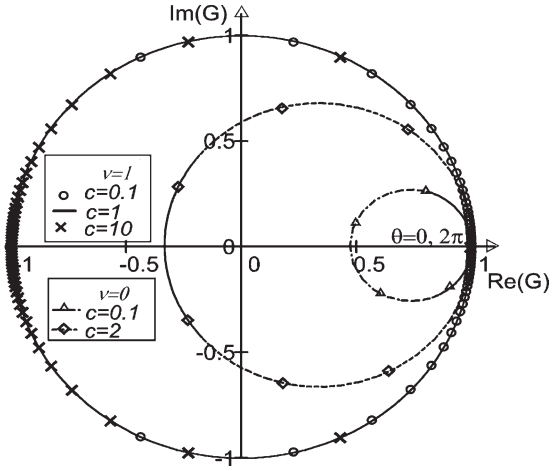

Figure 9 | Polar plot of the amplification factor for the SORD advection scheme.

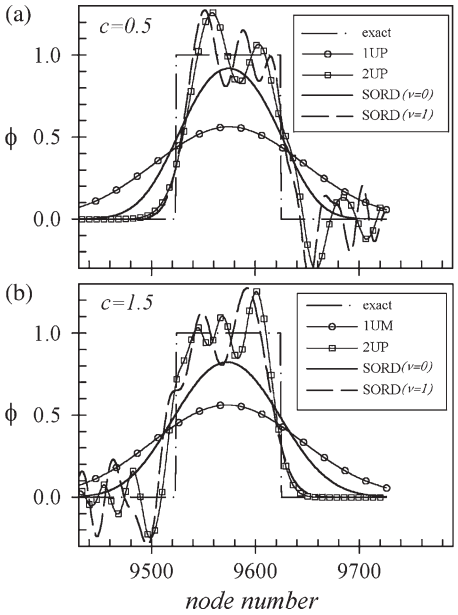

Figure 10 | Comparison of some advection schemes: marching SORD, first-order (1UM, 1UP) and second-order upwinding (2UP).

interval $0 \le c \le 2$. To increase the influence of the third-order schemes (and to improve dispersive properties of the resulting scheme) at the left and right sides of the interval, one can chose $\gamma = c/2$, leading to a new mixed-order method labeled as the Fourth-Order Reduced Dispersion (FORD). It is expected that the algorithm accuracy is almost fourth order at the center of the interval $0 \le c \le 2$, where the contribution of the constituent schemes is balanced, and approaches third order near the boundaries of the interval, where an influence of one of the third-order schemes becomes dominant. The single-step update for the scheme is given by

$$\begin{aligned}\left(\phi_i^{n+1}\right)_{adv}^{FORD} = &-\left[\frac{1}{12}c(1-c)(2-c)^2\right]\phi_{i+s}^n \\ &+\left[\frac{1}{6}c(1-c)(2-c)(3+3c-2c^2)\right]\phi_i^n \\ &+\left[\frac{1}{2}c(2-c)(1+2c-c^2)\right]\phi_{i-s}^n \\ &-\left[\frac{1}{6}c(1-c)(1+5c-2c^2)\right]\phi_{i-2s}^n \\ &+\left[\frac{1}{12}c^2(1-c)(2-c)\right]\phi_{i-3s}^n.\end{aligned} \tag{26}$$

The modulus of the amplification factor (Figure 11) suggests that the pure advection FORD is stable for $0 \le c \le 2$ and

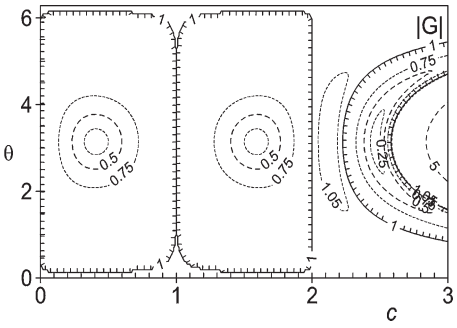

Figure 11 | Two-dimensional plot of the amplification factor modulus, $|G(\theta, c)|$, for the FORD advection scheme. Boundaries of the stability regions are marked with shading.

has a zone of "weak" instability at $2 < c \le 2.6$. Performance of some advective high-order schemes is shown in Figures 12 and 13 and Table 2 for different Courant numbers.

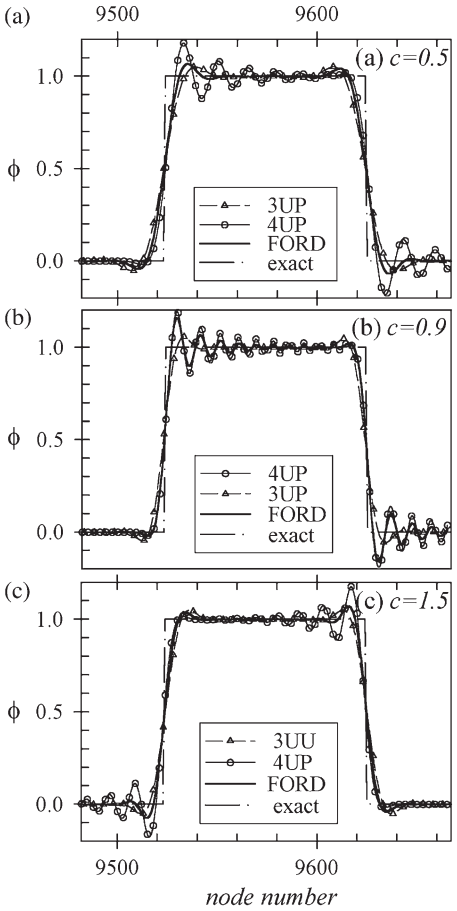

Figure 12 | Comparison of some advection schemes for different values of Courant number versus the exact solution. The compared schemes are FORD, third- (3UP = QUICKEST, 3UU) and fourth-order (4UP).

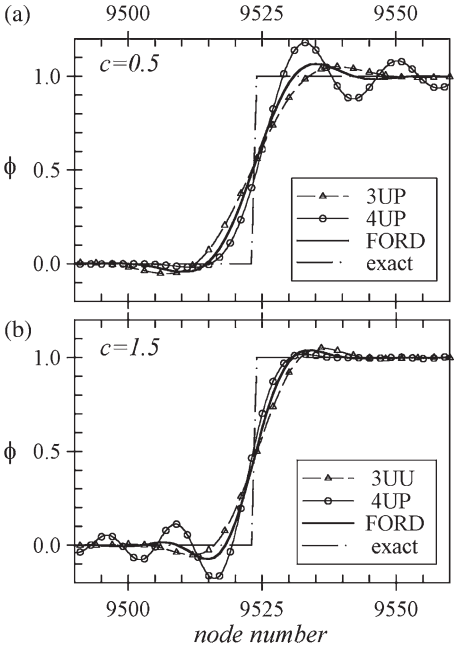

Figure 13 | Enlarged view. Comparison of some advection schemes for different values of Courant number versus the exact solution. The compared schemes are FORD, third- (3UP = QUICKEST, 3UU) and fourth-order (4UP).

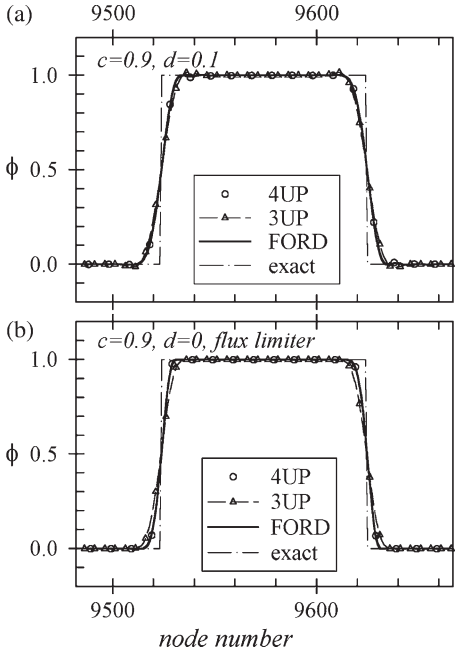

Figure 14 | Comparison of different methods for wiggling suppression in advection schemes: (a) using the diffusion term $d = 0.1\,m^2/s$; (b) using the flux limiter. 3UP = QUICKEST. $c = 0.9$.

Comparison shows that the fourth-order upstream (4UP) scheme has a leading phase error for $0 < c < 1$ and a lagging phase error for $1 < c < 2$, whereas FORD reduces the respective oscillation zones to $0.75 \le c < 1$ and $1 < c \le 1.25$, respectively. At the intervals $0 \le c \le 0.5$ and $1.5 \le c \le 2$ FORD has slightly more dispersive behavior than 3UP and 3UU schemes. The spurious oscillations increase as the Courant number tends to unity and reaches (4UP) maximum at $0.9 \le c \le 1.1$. The error measure of the FORD ($\varepsilon = 0.087$) is smaller than that of the third- and fourth-order upwinding ($\varepsilon = 0.111$ and $\varepsilon = 0.116$, respectively) near the left and right sides of the interval $0 \le c \le 2$, but is slightly larger than the error measure of third-order schemes near the center of the interval. Computations confirmed that, due to the conservative formulation (2), total mass of the scalar is conserved in every explicit scheme considered in this paper.

In many water quality problems, advection often dominates other phenomena, but turbulent diffusion seldom can be neglected. Following the above elaborated technique, advective FORD is combined with the diffusion approximation FTCS to yield an advection – diffusion scheme. Setting $D = 2\,m^2/s$ ($\Delta x = 100\,m$) in the test case is sufficient to extend the stability region of the combined scheme into the "weak" instability zone $2 < c \le 2.6$, thus making the algor-

Table 2 | Comparison of error measure, ε, for different numerical schemes using the test case

	$c = 0.9$		$c = 0.5, 1.5$	
Numerical schemes	**Pure advection**	**Advection + Diffusion**	**Advection + Flux limiter**	**Pure advection**
QUICKEST (3UP), 3UU	0.07161	0.08406	0.07272	0.11051
FORD	0.07664	0.06948	0.04944	0.08688
4UP	0.10102	0.06908	0.04877	0.11576

ithm stable at the entire interval $0 \leq c \leq 2.6$. Existence of the diffusion term improves not only stability, but also the phase behavior of high-order schemes. Setting the diffusion coefficient as low as $D = 0.1\,\mathrm{m}^2/\mathrm{s}$ in the test case decreases spurious oscillations of the QUICKEST significantly and eliminates wiggling of the FORD scheme entirely (Figure 14(a)). In fact, the diffusive term is almost as effective for wiggle suppression as the flux limiter of Leonard & Niknafs (1990) (Figure 14(b) and Table 2). If wiggles are suppressed, the error measure of FORD ($\varepsilon = 0.0494$) is just slightly higher that that of the fourth-order upwinding 4UP ($\varepsilon = 0.0488$), both leaving behind the third-order schemes ($\varepsilon = 0.0727$). Generally, computational tests show that the higher the order of schemes, the easier is the task of oscillation suppression and algorithm stabilization.

CONCLUSIONS

Employing the interpolation polynomial method, major high-order upwind advection–diffusion schemes are rederived and the recursive relationship (18) for an arbitrary-order advection scheme is established. Even though the third-order upwinding (QUICKEST) was once introduced as a rational basis for CFD, some features of the fourth-order upwinding (Equation (14)) appeal for attention. The main advantage of the scheme is the extended stability condition, with the local Courant number ranging from $0 \leq c \leq 2$ for a pure advection. It was thought that the major drawback of the fourth-order upwinding is in spurious oscillations, which generally are more severe for even-order schemes than for odd-order ones. It is shown in this paper that, if the diffusion term is present, the wiggles are smoothed out effectively even with a small value of the diffusion coefficient. Moreover, the large diffusivity may extend the stability range of some explicit high-order advection–diffusion schemes up to three units of the Courant number. For a pure advection, application of flux limiters is effective for wiggling suppression of (odd- or even-) high-order schemes. Generally, the higher the order of approximation, the easier is the task of scheme stabilization and oscillation elimination.

Stemming from the finding that higher-order schemes can be obtained from two lower-order methods using the recursive equation (18), manipulation with the interpolation variable offers a straightforward derivation technique of a new class of mixed-order schemes. Such schemes may inherit an extended stability range of even-order methods and improved dispersion behavior of odd-order ones. Two newly developed mixed-order schemes SORD (Equation (25)) and FORD (Equation (26)) demonstrate the desired qualities. The fourth-order upwind schemes (Equations (14) and (26)) show a potential to stand among the popular advective algorithms of computational hydraulics.

REFERENCES

Boris, J. P. & Book, D. L. 1973 Flux corrected transport I. SHASTA, A fluid transport algorithm that works. *J. Comput. Phys.* **11**, 38–69.

Courant, R., Friedrichs, K. O. & Lewy, H. 1928 Über die partiellen Differenengleichungen der mathematisches Physik. *Mathematische Annalen* **100**, 32–74.

Fromm, J. E. 1968 A method for reducing dispersion in convective difference schemes. *J. Comput. Phys.* **3**, 176–189.

Lax, P. D. & Wendroff, R. 1960 Systems of conservation laws. *Comm. Pure Appl. Math.* **13**, 217–237.

Lax, P. D. & Wendroff, R. 1964 Difference schemes with high order accuracy for solving hyperbolic equations. *Comm. Pure Appl. Math.* **17**, 381.

Leith, C. E. 1965 Numerical simulation of the Earth's atmosphere. *Meth. Comput. Phys.* **4**, 1–28.

Leonard, B. P. 1979 A stable and accurate convective modeling procedure based on quadratic upstream interpolation. *Comp. Meth. Appl. Mech. Engng.* **19**, 59–98.

Leonard, B. P. 1984 Third-order upwinding as a rational basis for computational fluid dynamics. In *Proc. Int. Comput. Techn. Appl. Conf (CTAC-83)* (eds B. J. Noye & C. Fletcher), pp. 106–120. Elsevier. New York.

Leonard, B. P. 1995 Order of accuracy of QUICK and related convection-diffusion schemes. *Appl. Math. Modell.* **19**, 640–653.

Leonard, B. P. 2002 Stability of explicit advection schemes. The balance point location rule. *Int. J. Numer. Meth. Fluids* **38**, 471–514.

Leonard, B. P. & Mokhtari, S. 1990 Beyond first-order upwinding: the ultra-sharp alternative for non-oscillatory steady-state simulation of convection. *Int. J. Numer. Meth. Engng.* **30**, 729–766.

Leonard, B. P. & Niknafs, H. S. 1990 The ultimate CFD scheme with adaptive discriminator for high resolution of narrow extrema. In *Proc. Int. Comput. Techn. Appl. Conf (CTAC-89)* (eds W. L. Hogarth & B. J. Noye), pp. 303–310. Hemisphere. New York.

Leonard, B. P., MacVean, M. K. & Lock, A. P. 1995 The flux integral method for multidimensional convection and diffusion. *Appl. Math. Modell.* **19**, 333–342.

Li, Yu & Rudman, M. 1995 Assessment of higher-order upwind schemes incorporating FCT for convection-dominated problems. *Numer. Heat Transfer B: Fundam.* **27** (1), 1–21.

Noye, B. J. 1986 Three point two-level finite difference methods for the one-dimensional advection equation. In *Proc. Int. Comput. Techn. Appl. Conf (CTAC-85)* (eds B. J. Noye & R. L. May), pp. 159–192. North-Holland. Amsterdam.

Roache, P. J. 1976 *Computational Fluid Dynamics*. Hermosa Publishers. Albuquerque, NM.

Roache, P. J. 1992 A flux-based modified method of characteristics. *Int. J. Numer. Meth. Fluids* **15**, 1259–1275.

Roe, P. L. 1986 Characteristic-based schemes for the Euler equations. *Ann. Rev. Fluid Mech.* **18**, 337–365.

Van Leer, B. 1974 Toward the ultimate conservative difference scheme. II. Monotonicity and conservation combined in a second-order scheme. *J. Comput. Phys.* **14**, 361–370.

Warming, R. F. & Beam, R. M. 1976 Upwind second-order difference schemes and applications in aerodynamics flows. *AIAA Journal* **24**, 1241–1249.

Zalesak, S. T. 1979 Fully multidimensional flux-corrected transport algorithms for fluids. *J. Comput. Phys.* **31**, 335–362.

APPENDIX A

List of right-hand face values for the advective term approximation

$$(\phi_r)^{1UP} = \phi_i^n$$

$$(\phi_r)^{2CN} = \left[\frac{1}{2}(1-c)\right]\phi_{i+1}^n + \left[\frac{1}{2}(1+c)\right]\phi_i^n$$

$$(\phi_r)^{2UP} = \left[\frac{1}{2}(3-c)\right]\phi_i^n - \left[\frac{1}{2}(1-c)\right]\phi_{i-s}^n$$

$$(\phi_r)^{3UP} = \left[\frac{1}{6}(1-c)(2-c)\right]\phi_{i+s}^n + \left[\frac{1}{6}(1+c)(5-2c)\right]\phi_i^n - \left[\frac{1}{6}(1-c^2)\right]\phi_{i-s}^n$$

$$= \frac{1}{2}\left(\phi_{i+s}^n + \phi_i^n\right) - \frac{c}{2}\left(\phi_{i+s}^n - \phi_i^n\right) - \frac{1-c^2}{6}\left(\phi_{i+s}^n - 2\phi_i^n + \phi_{i-s}^n\right)$$

$$(\phi_r)^{3UU} = \left[\frac{1}{6}(c^2-6c+11)\right]\phi_i^n - \left[\frac{1}{6}(2c^2-9c+7)\right]\phi_{i-s}^n + \left[\frac{1}{6}(c^2-3c+2)\right]\phi_{i-2s}^n$$

$$(\phi_r)^{4UP} = \left[\frac{1}{24}(1-c)(2-c)(3-c)\right]\phi_{i+s}^n + \left[\frac{1}{24}(1+c)(3c^2-17c+26)\right]\phi_i^n - \left[\frac{1}{24}(10-3c)(1-c^2)\right]\phi_{i-s}^n + \left[\frac{1}{24}(2-c)(1-c^2)\right]\phi_{i-2s}^n$$

$$(\phi_r)^{FORD} = -\frac{1}{12}\left[c^3-5c^2+8c-4\right]\phi_{i+s}^n + \frac{1}{12}\left[c^3-13c^2+12c+10\right]\phi_i^n - \frac{1}{12}\left[3c^2-11c^2+6c+2\right]\phi_{i-s}^n + \frac{1}{12}c\left[c^2-3c+2\right]\phi_{i-2s}^n.$$

List of right-hand pseudo-gradient values for the diffusive term approximation

$$(\phi_r')^{FTCS} = \phi_{i+1}^n - \phi_i^n$$

$$(\phi_r')^{2CN} = \phi_{i+1}^n - \phi_i^n$$

$$(\phi_r')^{2UP} = \phi_i^n - \phi_{i-s}^n$$

$$(\phi_r')^{3UP} = (1-c)\phi_{i+s}^n - (1-2c)\phi_i^n - c\phi_{i-s}^n$$

$$(\phi_r')^{3UU} = (2-c)\phi_i^n - (3-2c)\phi_{i-s}^n + (1-c)\phi_{i-2s}^n$$

$$(\phi_r')^{4UP} = \left[\frac{1}{12}(6c^2-18c+11)\right]\phi_{i+s}^n - \left[\frac{1}{4}(6c^2-14c+3)\right]\phi_i^n + \left[\frac{1}{4}(6c^2-10c-1)\right]\phi_{i-s}^n - \left[\frac{1}{12}(6c^2-6c-1)\right]\phi_{i-2s}^n$$

$$(\phi_r')^{FORD} = \left[\frac{1}{6}(6c^2-15c+8)\right]\phi_{i+s}^n - \left[\frac{1}{6}(18c^2-39c+12)\right]\phi_i^n + \left[\frac{1}{2}(6c^2-11c+2)\right]\phi_{i-s}^n - \left[\frac{1}{6}(6c^2-9c+2)\right]\phi_{i-2s}^n.$$

APPENDIX B. BOUNDARY CONDITIONS

Consider Equation (2) to be valid in a domain, having a left boundary at node with zero index, as in Figure B.1. The cell-average of the transported scalar ϕ at the cell at the nth time-level can be identified as ϕ_0^n, and two neighboring points from left and right are ϕ_{-1}^n and ϕ_1^n, respectively. Depending on the type of boundary condition, one can prescribe a cell-average value f_B, or normal (to the boundary) derivative f_B', or weighted average of both at the boundary.

The ***Dirichlet boundary condition*** specifies the value of the transported scalar at the boundary as $\phi = f_B$, leading to

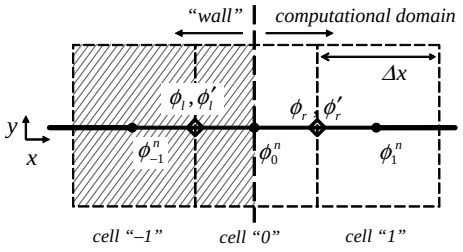

Figure B.1 | Sketch of computational cells near the boundary.

the set of relationships

$$\phi_0^{n+1} = f_B, \quad \phi_l = f_B, \text{ and } \phi_l' = \phi_r'. \tag{B.1}$$

The ***Neumann boundary condition*** specifies the normal derivative of the transported scalar on the boundary surface as $\partial\phi/\partial x = f_B'$. The latter can be approximated as

$$\phi_0^{n+1} = f_r, \quad \phi_l = \phi_r, \text{ and } \phi_l' = f_B'. \tag{B.2}$$

It is important to stress that conditions (B.1) and (B.2) are as accurate as the relationship (2) itself. Therefore, accuracy of the entire boundary value problem (2), (B.1) and (B.2) depends only on chosen approximations of the advection and diffusion terms (given in Appendix A).

APPENDIX C. AN EXAMPLE OF MULTIPLE SOLUTIONS OCCURRING DURING BACK-TRACKING IN SEMI-LAGRANGIAN SCHEMES

Consider a one-dimensional positive flow given by velocity values $\{u_{i-3}, u_{i-2}, u_{i-1}, u_i\} = \{3, 2, 1, 0\}$ upstream of the ith node, as shown in Figure C.1. Concrete values are given for

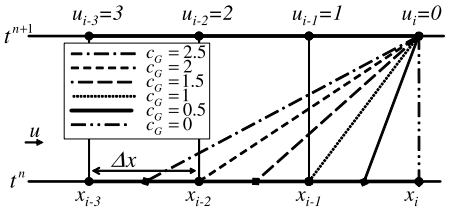

Figure C.1 | Example of multiple solutions occurred during back-tracking in semi-Lagrangian schemes.

the illustrative purpose only, as similar reasoning is valid for any non-uniform flow. A backtracking procedure can be started keeping in mind the application of one of the first-order accurate schemes, say, 1UP or 1UU. There is an equal opportunity to arrive at the point (t^{n+1}, x_i) from the departure interval $[x_{i-1}, x_i]$ using the averaged velocity $\bar{u}$ computed as $(u_{i-1} + u_i)/2$, leading to the "global" Courant number $c_G = 0.5$; from the interval $[x_{i-2}, x_{i-1}]$ with the "global" Courant number $c_G = 1.5$, and from the interval $[x_{i-3}, x_{i-2}]$ with $c_G = 2.5$. In all the above cases the "local" Courant number is equal to 0.5. If the target scheme is expected to be an upwind second-order, the sought stencil and averaged velocity has to include three nodes at intervals $[x_{i-2}, x_i]$ or $[x_{i-3}, x_{i-1}]$, leading to $c_G = 1$ and $c_G = 2$, respectively. The third-order up-upwind scheme (3UU) would end up with the arithmetic-averaged velocity $\bar{u} = (3 + 2 + 1 + 0)/4$ and trajectory starting at $c_G = 1.5$. The trend is clear, that a back-tracking procedure depends strongly on the assumed stencil and underlying advection approximation method, and may lead to multiple solutions for non-uniform flows. In such cases, mass conservation in semi-Lagrangian schemes is not guaranteed.